J Polym Res (2016) 23: 241
DOI 10.1007/s10965-016-1140-0

ORIGINAL PAPER

Study on the synergistic effect of clinoptilolite on the swelling kinetic and slow release behavior of maize bran-based superabsorbent nanocomposite

Ali Olad[1] · **Hamed Gharekhani**[1] · **Abdolreza Mirmohseni**[1] · **Ahmad Bybordi**[2]

Received: 30 May 2016 / Accepted: 9 November 2016 / Published online: 17 November 2016

Abstract A new type of maize bran (MB)-based superabsorbent nanocomposite with fertilizer slow-release property was synthesized by free-radical graft copolymerization of acrylic acid (AA) and acrylamide (AAm) monomers onto MB backbone in the presence of clinoptilolite (clino) and NPK fertilizer compound. The FTIR results indicated that the grafting reaction and the nanocomposite formation have been performed, successfully. Rheological analyses were done to evaluate the stability of the three-dimensional cross-linked gel network of synthesized hydrogels. The effect of variable factors such as salt solution type and concentration, and solution pH on the water absorbency of hydrogel samples was investigated. Also, swelling kinetic studies for all hydrogel samples were performed. Rheological measurements revealed that all hydrogel samples had a strong gel framework with stable crosslinked network. Moreover, superabsorbent nanocomposite showed higher gel strength compared with neat hydrogel which was due to the additional physical crosslinking effect of clino particles. The equilibrium water absorption capacity of the synthesized hydrogels in all saline solutions was lower than that of values in distilled water. Additionally, hydrogel samples showed pH-sensitive swelling behavior. Fertilizer release studies showed that NPK loaded superabsorbent nanocomposite possesses excellent slow-release behavior. Besides, it had better water retention capacity in soil. These results revealed that the superabsorbent nanocomposite with good slow-release and water retention properties, being cost effective and environment-friendly can efficiently improve the utilization of fertilizer and water resources in agricultural and horticultural applications.

Keywords Slow-release fertilizer formulation · Superabsorbent nanocomposite · Maize bran · Clinoptilolite · Water retention

✉ Ali Olad
a.olad@yahoo.com

[1] Polymer Composite Research Laboratory, Department of Applied Chemistry, Faculty of Chemistry, University of Tabriz, Tabriz, Iran

[2] Soil and Water Research Department, East Azarbaijan Agricultural and Natural Resources Research Center, AREEO, Tabriz, Iran

Introduction

Fertilizer and water are the vital input materials that limit the production of agricultural crops, thus effective utilization of them is an important issue [1]. Depending on application method and soil conditions, about 30–70 % of nutrients of the applied conventional fertilizers is lost to the environment and cannot reach to the target plant, resulting in large economic and resource loss as well as serious environmental pollution [2, 3]. An effective way to mitigate nutrient loss is to develop slow-release fertilizer (SRF) formulations, which keep fertilizer concentration at an active level in soil by liberating nutrients coincide with plant requirements. These SRF formulations exhibit many advantages over the conventional types, such as reducing the frequency of application, decreasing fertilizer loss, sustainable supplying of the nutrients, and alleviating environmental pollution concerns [4, 5]. At the same time, due to the scarcity of water resources, irrigation water consumption must be managed, effectively. One of the most important materials used as polymeric matrix in fabrication of SRF formulations is superabsorbent hydrogel (SAH). SAHs are three-dimensionally cross-linked hydrophilic polymers that can absorb and retain a large amount of water or aqueous solutions [6, 7]. Therefore, their utilization in agriculture field can exhibit encouraging results such as reducing irrigation water consumption, improving

fertilizer retention in soil, enhancing the plant growth rate, and mitigating environmental pollution caused by water-soluble fertilizers [8]. Since most of SAHs are based on the synthetic acrylate monomers, thus their high production cost and nonbiodegradability are key issues facing extensive development of them in agriculture field [9]. In contrast, natural polysaccharides such as starch [10], chitosan [11], carboxymethyl celloluse (CMC) [12], and alginate [13], due to abundance, non-toxicity, biocompatibility, and biodegradability have been used widely as useful SAH materials [14, 15].

Nevertheless, the use of maize bran (MB) as most cost-effective resource of starch for synthesis of SAHs has been received little attention. The adoption of MB as SAH material not only provides a new insight in effective utilization of crop residues, but also improves biodegradation property of SAHs [16]. In spite of the special advantages of hydrogels in agrochemical field, the high production cost makes their practical application infeasible. To solve this problem, intense efforts have been devoted to synthesize nanocomposite hydrogels with clay minerals such as montmorillonite (MMT) [17], attapulgite [18], kaolin [19], and bentonite [20]. Among the clay minerals, clinoptilolite (clino), due to the precious physicochemical features such as high ion exchange capacity, large surface area, dehydration activity, and low cost has attained much attention in agricultural applications [21]. Incorporation of clino into hydrogel network not only can reduce final production cost but also can improve swelling property, mechanical, and thermal stability of the prepared hydrogel nanocomposite [22].

Encouraging results obtained by incorporation of clino with MB-g-P(AA-co-AAm) (Hyd) SAH, promoted us to develop a new type of slow release fertilizer formulation through graft copolymerization of acrylic acid (AA), and acrylamide (AAm) monomers onto MB backbone in the presence of clino and NPK fertilizer compound. The swelling kinetic of the prepared hydrogels as well as the influence of different salt and pH solutions on the swelling behavior of Hyd and Hyd/clino samples was investigated. The fertilizer release behavior and the fertilizer release kinetics of the NPK loaded hydrogel samples were also studied.

Experimental

Materials

MB was purchased from Mahshad company in Yazd, Iran and was used without further purification. Acrylic acid (AA), acrylamide (AAm), N,N'-methylene bisacrylamide (MBA), ammonium persulfate (APS), urea, potassium dihydrogen phosphate, ammonium dihydrogen phosphate, and acetone were purchased from Merck company. Clino was supplied from the Meianah mine in East Azerbaijan, Iran. Dialysis membrane bag (with a molecular cut-off of 12400) was purchased from Sigma-Aldrich (USA). Other agents used in this study possessed analytical grade and all solutions were prepared with distilled water.

Preparation of Hyd/clino superabsorbent nanocomposite

First, a proper amount of grounded MB (particle size = 40–80 mesh) along with the appropriate amount of clino (0.5–8 wt%, with respect to MB) were poured into a beaker containing 30 mL distilled water, and then were sonicated at 50 W power for 3 min. Thereafter, the resultant suspension was transferred into a 250 mL four-necked round-bottom flask equipped with a mechanical stirring rod, a reflux condenser, a thermometer, and a nitrogen line. With stirring, 2 g AAm was added into the mixture and temperature was raised gradually to 40 °C using a water bath. Then, a mixed solution of partly neutralized (70 %) AA (7 mL) and MBA (1 wt%, with respect to MB) was slowly dropped into the reaction mixture. After purging with nitrogen to eliminate the dissolved oxygen, a determined amount of APS (10 wt%, with respect to MB) was charged into the flask to initiate graft copolymerization reaction. The reaction mixture was heated to 70 °C, and kept for 3 h under nitrogen atmosphere to complete the polymerization reaction. Afterwards, the resultant gel product was cooled to room temperature and after cutting into small pieces, immersed in ethanol for 24 h to remove residual unreacted species. The crud product was dried in a vacuum oven at 70 °C for 24 h, and then was milled and screened using 40–80 mesh sieves. As comparison, the Hyd sample without clino was synthesized similar to the above described procedure.

Preparation of slow-release fertilizer (SRF) formulation

To synthesize NPK SRF formulation, proper amounts of urea (10 g), ammonium dihydrogen phosphate (5 g), and potassium dihydrogen phosphate (5 g) were fed into a stirring reaction mixture, and then polymerization process was carried out similar to the previously described method.

Characterization

The chemical structure of the samples was analyzed using a FTIR spectroscopy (FTIR, Bruker Tensor 27) in the wavenumber range of 400–4000 cm^{-1}. Prior to the measurement, the well dried and powdered samples were mixed with KBr powder, and then compressed into a pellet for FTIR characterization. XRD measurements were carried out using a X-ray diffractometer (Siemens AG, Karlsruhe, Germany) equipped with Cu Kα radiation source, and XRD patterns were recorded in the scattering angle range from 2 to 70°. Surface morphology of the hydrogel samples was also studied using a MIRA3 FEG-SEM (Tescan, Czech) scanning electron microscope instrument.

Property investigation

Measurement of percentage grafting efficiency and gel content

The grafting efficiency (GE) percent which describes the percentage of grafted polymer onto stock polymer was determined as follows. First, a pre-determined amount of graft copolymer was extracted with acetone for 24 to remove any unreacted species. After drying the extracted gel product in a vacuum oven at 70 °C for 24 h, it was weighed accurately to calculate GE (%) using the following equation [23]:

$$GE(\%) = \frac{W_3 - W_1}{W_2 - W_1} \times 100 \quad (1)$$

Where W_1 (g) is weight of MB, W_2 (g) and W_3 (g) are weight of the grafted MB copolymer before extraction and after extraction, respectively.

Gel content (GC) of a hydrogel sample which defines its insoluble part in deionized water was determined as follows. A given amount of dry hydrogel sample (W_0) was immersed entirely in deionized water for 48 h at room temperature. Thereafter, the extracted hydrogel sample was dried in a vacuum oven at 80 °C for 24 h to a constant weight (W_1). The gel fraction was then measured using the following equation [24]:

$$GC(\%) = \left(\frac{W_1}{W_0}\right) \times 100 \quad (2)$$

Rheological analysis

The viscoelastic properties of crosslinked Hyd and Hyd/clino samples were investigated using a Paar-Physica oscillatory rheometer (MCR300, Germany) at 25 °C with parallel plates of 25 mm diameter and gap of 1 mm. A strain sweep test at frequency of $\omega = 10$ Hz was first executed to find the linear viscoelastic (LVE) range, in which storage modulus (G′) and loss modulus (G″) are independent of the strain amplitude. It was found that below 0.5 % deformation, G′ and G″ of synthesized hydrogels are independent of the applied strain, indicating the LVE behavior. Thereafter, to study the viscoelastic performance of the hydrogels, frequency-sweep tests at a constant strain ($\gamma = 0.5$) were performed over the frequency range 0.1–100 Hz.

Measurement of equilibrium water absorbency and swelling kinetics

To perform swelling kinetic studies, a known amount (W_d) of dried hydrogel sample was soaked in 100 mL distilled water at room temperature. Thereafter, the weight of swollen hydrogel sample (W_t) was measured at certain time intervals (t). All swelling measurements were carried out in triplicate and average values were recorded. At equilibrium swelling ratio, the weight of the swollen hydrogel sample is fixed at a constant value (W_e). The swelling ratio (Q_t) and equilibrium swelling ratio (Q_{eq}) were calculated using the following equations:

$$Q_t\left(g/g\right) = \frac{W_t - W_d}{W_d} \quad (3)$$

$$Q_{eq}\left(g/g\right) = \frac{W_e - W_d}{W_d} \quad (4)$$

To investigate the swelling behavior of the synthesized hydrogel samples in different salt solutions, various saline solutions (NaCl, $CaCl_2$, and $FeCl_3$) with different concentrations were chosen as swelling medium. The equilibrium water absorbency was determined similar to the earlier described method.

To assess the swelling behavior of the synthesized hydrogel samples at various pH values, different acidic or basic solutions prepared by diluting aqueous solutions of NaOH (0.1 M) and HCl (0.1 M) were adopted as swelling medium. The equilibrium swelling ratio was calculated according to the above mentioned procedure.

Fertilizer release studies in water

A pre-determined amount of NPK loaded hydrogel sample (0.05 g) was placed in a dialysis membrane bag and the bag was tightly closed by knotting its two ends. This system was immersed in 100 mL distilled water, and then was stirred continuously at room temperature (25 °C) using a magnetic stirrer throughout the release analyses. At given time intervals, 10 mL of the solution containing released fertilizer was withdrawn and 10 mL fresh distilled water was added to keep the solution volume constant. All release experiments were performed three times, and average values were considered. The fertilizer concentration in the withdrawn solution was determined by measuring its conductivity, and finally cumulative release was calculated using the following equation:

$$E = \frac{V_E \sum_1^{n-1} C_i + V_0 C_n}{m_0} \times 100 \quad (5)$$

Where E is the accumulative release (%) of NPK fertilizer, V_E and V_0 (mL) are the sampling volume and the initial volume of release media, respectively. C_i and C_n are the fertilizer concentrations (mg/mL), i and n are the sampling times, and m_0 is the mass of fertilizer in the hydrogel samples (mg).

Fertilizer release studies in soil

To study the release behavior of the NPK loaded hydrogel samples in soil, 1 g fertilizer loaded hydrogel sample was

well-mixed with 100 g loamy sand soil (below 20 mesh), and then kept in a 200 mL glass beaker. Thereafter, it was moistened with 70 mL distilled water, and incubated at room temperature (25 °C). At certain time intervals (every 24 h), 10 mL solution was sampled for fertilizer determination, and then the same volume of fresh distilled water was introduced into the soil to keep its moisture content at a constant value. Finally, fertilizer concentration and cumulative release were calculated similar to the above described procedure.

Water retention capability of Hyd/clino/NPK formulation in soil

1 g dried Hyd/clino/NPK hydrogel sample was well-mixed with 100 g dry loamy sand soil (below 20 mesh), and then kept in a 250 mL plastic beaker. Thereafter, 50 mL distilled water was decanted into the beaker, and was weighed (W_0). A control experiment with no Hyd/clino/NPK (W) was also performed. The beakers were retained at room temperature (25 °C) and were weighed every day (W_t). The water retention (WR (%)) capacity of soil was calculated using the following equation:

$$WR(\%) = \frac{W_t - W}{W_0 - W} \times 100 \quad (6)$$

Results and discussion

Synthesis mechanism of superabsorbent nanocomposite

The superabsorbent nanocomposite was synthesized by free-radical graft copolymerization of AA and AAm monomers onto MB backbone in the presence of initiator (APS), crosslinking agent (MBA), and clino. Figure 1a illustrates the proposed graft copolymerization mechanism. Initially, thermal dissociation of APS molecules leads to generation of the sulfate anion-radicals which serve as initiators. These active radicals attack on the starch molecules, creating alkoxy radicals onto their chains which results in grafting of neighboring monomers on those active sites. During the chain propagation process, end vinyl groups of MBA may react synchronously with copolymer chains causing to formation of cross-linked hydrogel network. The final hydrogel network is made in the presence of clino particles which can act as physical cross-linking agent. The images of swollen hydrogel samples have been shown in Fig. 1b in which the photographs at left and right sides respectively are assigned to the hydrogel (Hyd) and hydrogel nanocomposite (Hyd/clino).

In the present study, the amount of GE (%) for superabsorbent nanocomposite (Hyd/clino) was about 99.5, which is higher than that of the corresponding value (98.8) for hydrogel sample. This is due to the interaction of hydroxyl groups on the surface of clino particles with the AA and AAm monomers which can improve the polymeric network [25]. Also, the amount of GC decreased from 95.19 % for hydrogel to 86.66 % for superabsorbent nanocomposite with incorporation of clino into hydrogel network. This is due to the additional physical cross-linking effect of clino particles which can lead to the more quickly gelation process compared to the neat hydrogel. Consequently, gel formation at very early stage of polymerization can cause to the enhanced water soluble parts, resulting in decreased GC.

Characterization

FTIR spectroscopy

FTIR spectroscopy was used to characterize the structure and molecular interactions of functional groups of the synthesized hydrogels. The FTIR spectra of MB, clino, Hyd, Hyd/clino, Hyd/clino/NPK, and pure NPK fertilizer have been presented in Fig. 2. As shown in Fig. 2f for clino, the broad absorption band at 3446 cm^{-1} is attributed to the hydroxyl stretching vibration in Al–OH–Al and Si–OH–Si groups. Also, the peaks appeared at 1635 and 1049 cm^{-1} are related to the H–O–H bending and Si–O(Si),(Al) stretching vibrations, respectively. Additionally, stretching bridges of Si–O(Si) and Si–O(Al) groups were appeared as two distinct absorption bands at 796 and 607 cm^{-1}, respectively [26]. In FTIR spectra of MB (Fig. 2a), the broad absorption band appeared at approximately 3420 cm^{-1} is assigned to the –OH stretching vibration of the glucose unit, while peaks at 1035, 1079, and 1163 cm^{-1} are attributed to C–O stretching vibration of the glucose unit in the starch molecule structure. Also, absorption bands at 1382 and 1461 cm^{-1} related to the O–H in-plane bending vibration of the glucose unit appeared as two individual peaks [8]. Moreover, a sharp peak observed at 2926 cm^{-1} is related to the stretching vibration of C–H bond [16]. As can be seen from IR spectra of Hyd (Fig. 2b), Hyd/clino (Fig. 2c), and Hyd/clino/NPK (Fig. 2d) the absorption bands appeared at approximately 1678, 1606, and 1622 cm^{-1} are related to the overlapped stretching vibration of the carbonyl groups of AA and AAm as well as the N–H bending mode [27]. Also, the intense absorption bands of O–H and N–H groups were emerged between 3300 and 3500 cm^{-1} which have overlapped together. Furthermore, the absorption bands appeared in wavenumber range of 1150–1350 cm^{-1} are assigned to stretching vibration of C–N and C–O groups as well as bending mode of O–H bond [28]. Two sharp peaks observed between 2850 and 2980 cm^{-1} are attributed to the combined stretching vibration of CH_2 groups in both AA and AAm in hydrogel structure [29]. The characteristic absorption bands of the C–O group of glucose units in starch molecule have appeared with slight shift in IR spectra of Hyd, Hyd/clino, and

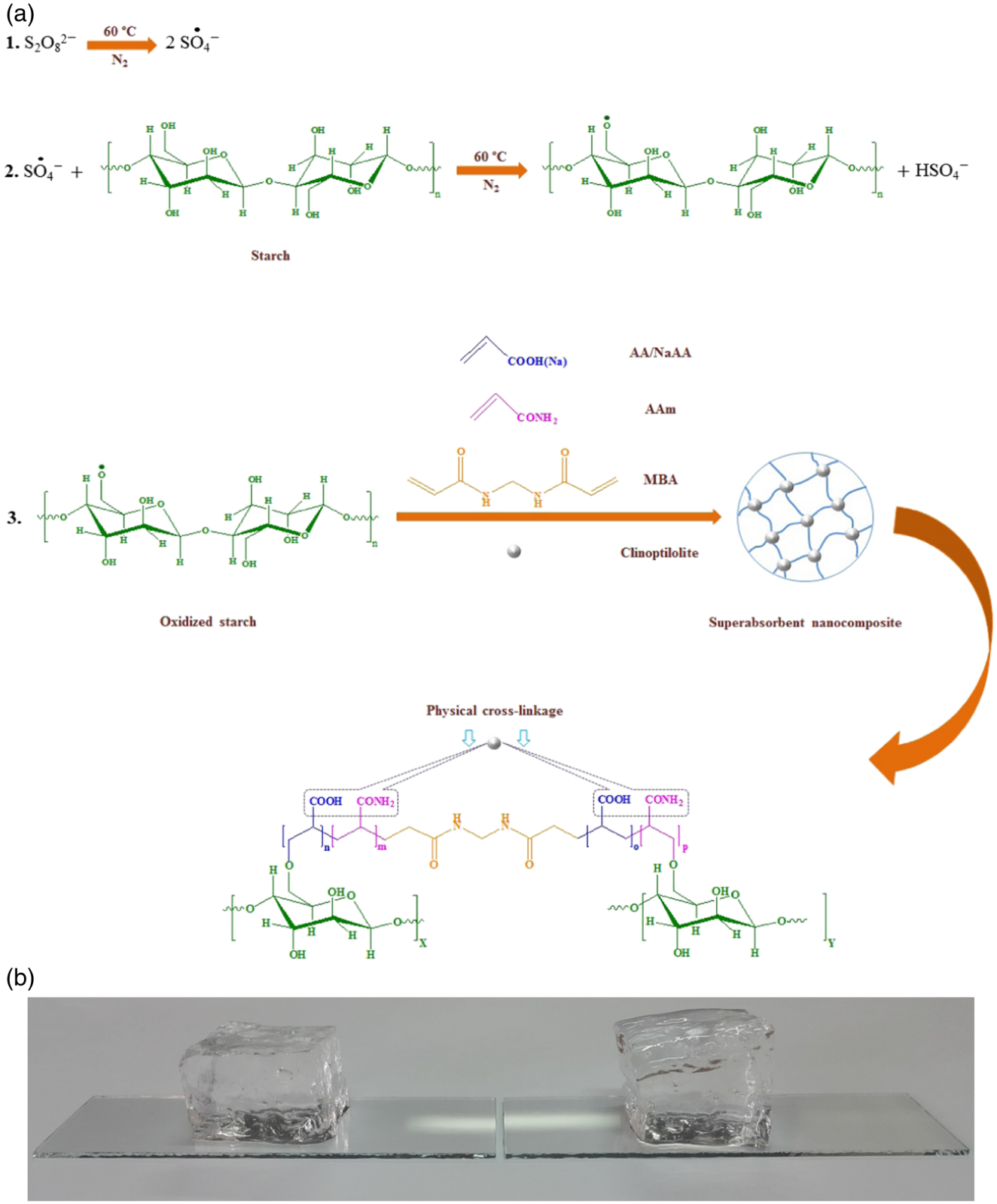

Fig. 1 Proposed graft copolymerization mechanism for synthesis of MB-g-poly (AA-co-AAm)/clino hydrogel nanocomposite (**a**), and photographs of hydrogel (Hyd) (*left*) and hydrogel nanocomposite (Hyd/clino) (*right*) samples (**b**)

Hyd/clino/NPK samples, confirming the effective grafting of AA and AAm monomers onto MB backbone [16]. In addition, the characteristic absorption band of Si–O group in clino structure has appeared in IR spectra of Hyd/clino and

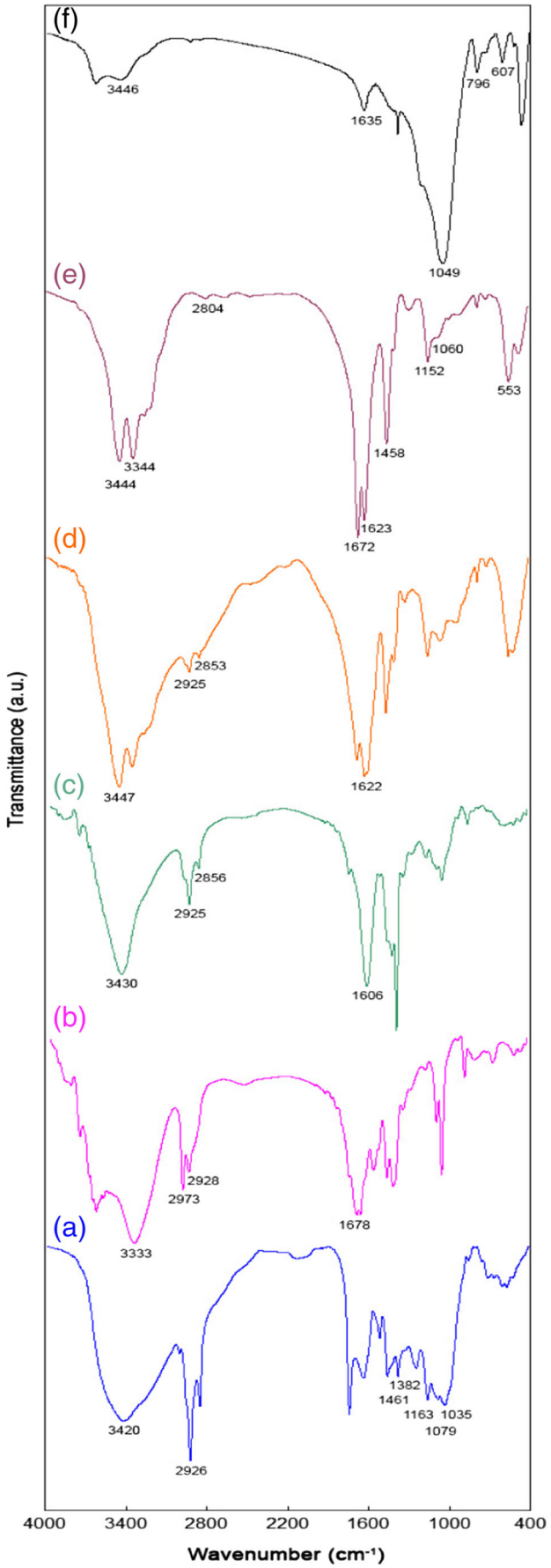

◀ **Fig. 2** The FT-IR spectra of MB (**a**), Hyd (**b**), Hyd/clino (**c**), Hyd/clino/NPK (**d**), NPK (**e**), and clino (**f**)

Hyd/clino/NPK samples which is an evidence for successful incorporation of clino into the hydrogel network. As shown in Fig. 2e for pure NPK fertilizer, two absorption bands observed at 3344 and 3444 cm^{-1} are assigned to the symmetric and asymmetric stretching modes of the NH_2 groups in urea molecule. Moreover, the sharp peak emerged at 1600 to 1700 cm^{-1} is related to the carbonyl stretching vibration of urea [30]. The peaks appeared at 2804, 1458, 1152, and 1060 cm^{-1} are corresponded to the O–H stretching, the P=O stretching, the P–OH stretching, and the HO–P–OH bending, respectively. Also, the absorption band of PO_4 group is observed as an almost sharp peak at 553 cm^{-1}. The characteristic absorption bands of ammonium dihydrogen phosphate have appeared between 700 and 900 cm^{-1} ascribing to the stretching vibration of O–N=P and $–ONO_2$ groups [29]. Comparing with the IR spectra of Hyd/clino, the characteristic absorption bands of pure NPK fertilizer have emerged with slight shift in IR spectra of Hyd/clino/NPK which confirm well encapsulation of NPK fertilizer compound within superabsorbent nanocomposite.

XRD patterns analysis

To investigate the structure and crystallinity of the materials, XRD patterns of the clino, Hyd, Hyd/clino, and Hyd/clino/NPK were recorded and provided in Fig. 3. The diffraction peaks of clino (Fig. 3a) appeared at $2\theta = 9.85°$, 11.19°, and 22.4° are attributed to the Miller indices of [020], [200], and [400], respectively [21]. These peaks confirm its crystalline structure. The appearance of two weak broad peaks at $2\theta =$ 22° and $2\theta = 38°$ in XRD patterns of Hyd (Fig. 3b) and Hyd/clino (Fig. 3c) is an evidence for their amorphous nature [22].

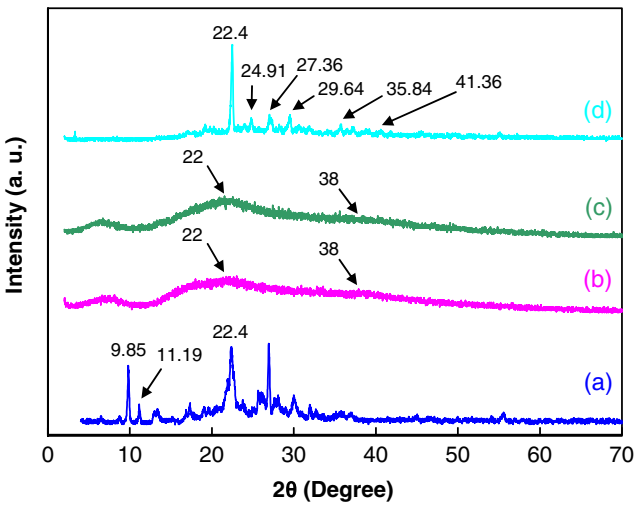

Fig. 3 The XRD patterns of clino (**a**), Hyd (**b**), Hyd/clino (**c**), and Hyd/clino/NPK (**d**)

However, due to the overlapping of amorphous broad peaks of Hyd component with characteristic peaks of clino in nanocomposite composition, typical crystallite reflections of the clino component have not emerged in XRD pattern of Hyd/clino sample. According to the XRD pattern of Hyd/clino/NPK (Fig. 3d), peaks related to the clino and Hyd components have shifted slightly to higher degrees which can be related to the incorporation of NPK compound into hydrogel nanocomposite network.

Surface morphology analysis

The surface morphologies of Hyd, Hyd/clino, and Hyd/clino/NPK samples were investigated through SEM images (Fig. 4). It can be observed that Hyd sample (Fig. 4a) has a relatively smooth and lamellar morphology which do not provide more pores for it. However, in the presence of clino, due to its physical crosslinking effect, highly porous network structures are formed which can be obviously seen in SEM images of Hyd/clino sample (Fig. 4b and c). These interlinked porous structures increase the contact surface area, leading to easier and faster diffusion of water molecules into hydrogel network, which finally induce a larger improvement in water uptake capacity and water absorption rate compared with the neat hydrogel. Besides, incorporation of clino into hydrogel network caused that spherical-like polymeric structures (with dimensions lower than 100 nm) form within hydrogel matrix, as shown in SEM image of Hyd/clino sample with higher magnification (Fig. 4d). As shown in Fig. 4e and f for Hyd/clino/NPK, the crystals of

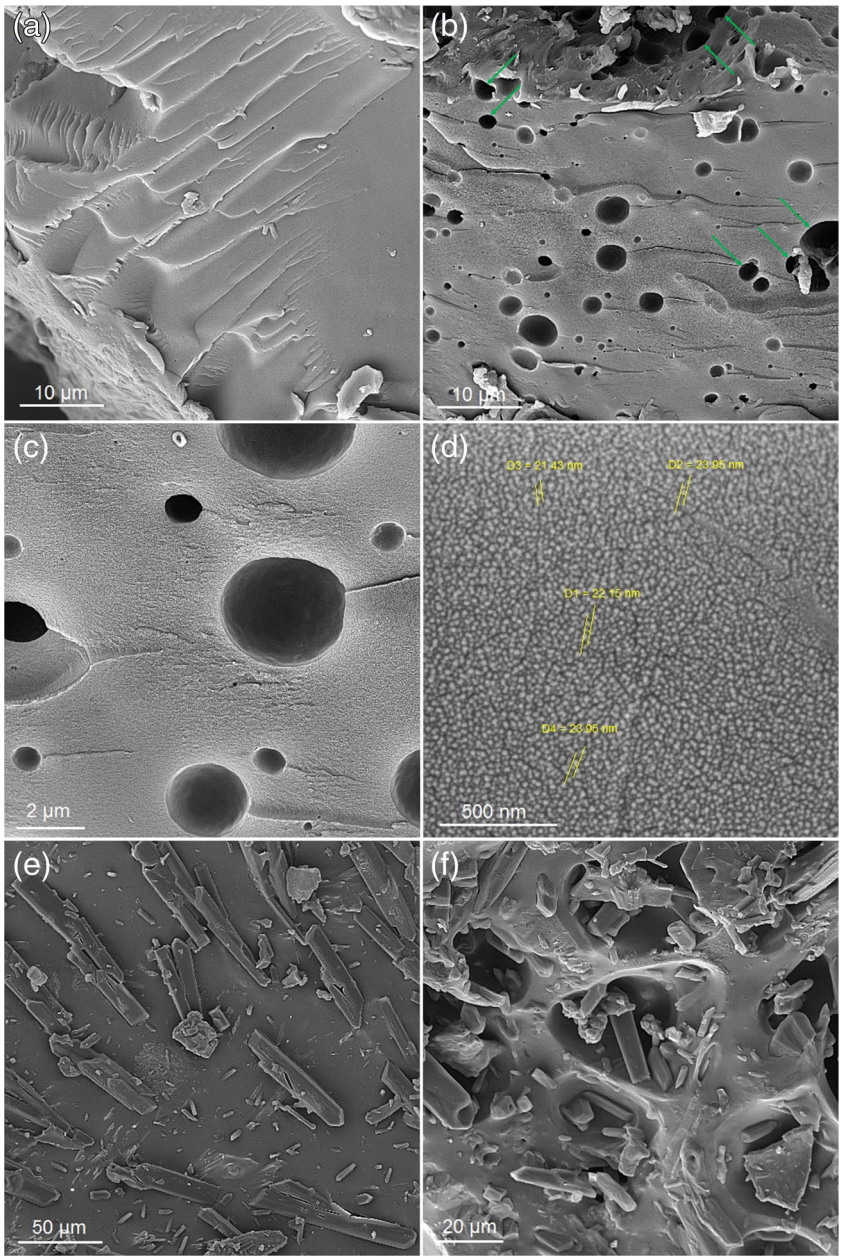

Fig. 4 SEM images of Hyd (with 1 wt% MBA content) (**a**), Hyd/clino (with 2 wt% clino content) (**b**-**d**), and freeze-dried Hyd/clino/NPK (**e**) and (**f**)

urea, potassium dihydrogen phosphate, and ammonium dihydrogen phosphate in NPK fertilizer composition have been distributed finely onto the surface and also within the pores of the hydrogel nanocomposite. As it is clear, the interconnected pores in Hyd/clino/NPK network can delay dissolution and subsequently diffusion of the loaded fertilizer into swelling medium, and thus can control the release rate of fertilizer. As a result, incorporation of clino into hydrogel network not only can cause hydrogel absorb larger amounts of water in short time periods but also can regulate the fertilizer release behavior.

Rheological measurements

To study the gel properties as well as the stability of three-dimensional crosslinked hydrogel network of Hyd and Hyd/clino samples, rheological analyses were performed by measuring the mechanical response of the samples versus oscillatory frequencies ranging from 0.1 to 100 Hz. Prior to frequency-sweep experiments, strain-sweep tests at constant frequency ($\omega = 10$ Hz) (Fig. 5a) were carried out on the hydrogel samples to determine the linear viscoelastic (LVE) region, where G′ (storage modulus) and G″ (loss modulus) are independent of the applied strain. As can be clearly seen from Fig. 5a, the strain amplitude was determined as 0.5 %. The plots of G′ and G″ versus oscillatory frequencies have been shown in Fig. 5b. According to Fig. 5b, the values of G′ and G″ for hydrogel samples showed relatively an increasing trend over the all frequency range. Also, G′ values remained almost constant in the frequency range of 0.41–18.9 Hz, indicating the frequency-independent feature of storage modulus of hydrogels. Moreover, the values of G′ were greater than that of G″ throughout the whole frequency range, which is an indicative of predominant elastic nature of hydrogels over their viscous nature. These characteristics revealed that all hydrogel samples had stable three-dimensional crosslinked network, and thus could form strong gel frameworks. The results also showed that Hyd/clino sample had higher G′ values compared with the Hyd sample in all frequency range, implying its stiffest gel network. Besides, G″ of Hyd/clino sample reached to 32.7 Pa at frequency of 100 Hz, demonstrating 20.4 % reduction compared to the initial G″ value at 0.1 Hz. While, for Hyd sample, G″ exhibited an increase of 94.5 % at the end frequency value. These observations again suggested that Hyd/clino was the strongest gel network. The reason for this phenomenon can be elucidated as follows. The strong mutual interactions between clino particles and polymeric component of hydrogel nanocomposite led to formation of additional physical crosslinking points within hydrogel network. These physical cross-linkages make polymer chain segments capable to pack together tightly, and thus build stiff gel frameworks that presented higher storage modulus.

As it is clear, G′ values of Hyd/clino sample sharply increased at high frequencies (low relaxation times). This can be interpreted by the poor rearrangement capability of longer polymer chains of hydrogel nanocomposite at high frequencies. On the other hand, at higher frequencies, longer polymer chains (with large relaxation times) cannot rearrange themselves in the time period of imposed movement [31]. Therefore, the polymer chains of Hyd/clino become stiff, that identified by a sharp rise in G′ values. In contrast, Hyd sample showed a sudden fall in G′ values at high frequencies. This can be attributed to the lower gel strength of Hyd sample which caused to its structural break by mechanical shear.

Swelling studies

The effect of clino content on the swelling ratio of synthesized hydrogels in distilled water is found in Fig. 6a. As depicted in Fig. 6a, the water absorbency increases with increasing clino content until it acquired the highest value of 1153 g/g at 2 wt% clino content. Thereafter, the equilibrium water absorbency decreased with further increasing of clino content up to

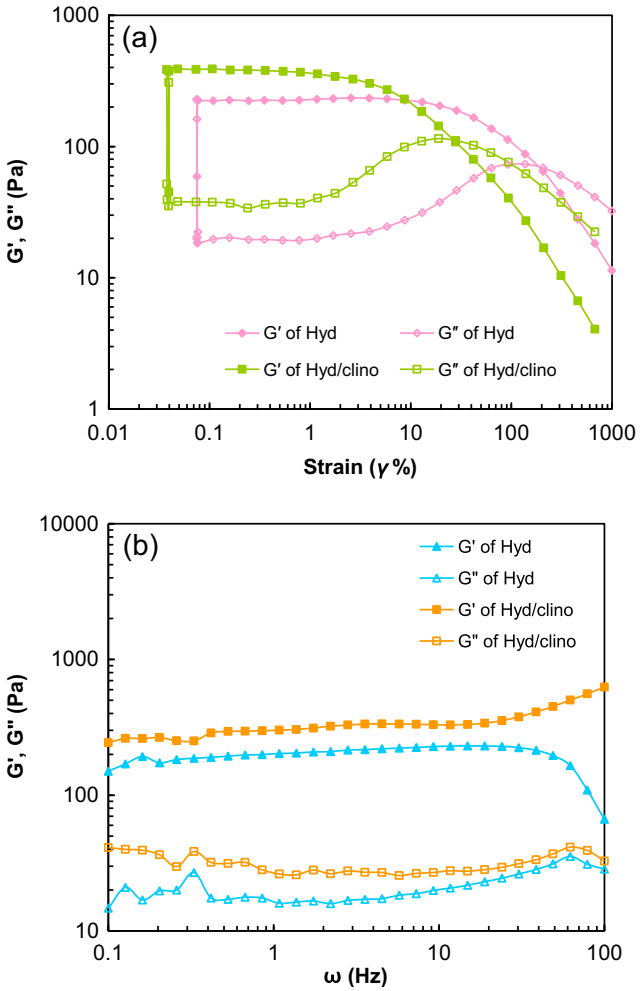

Fig. 5 Strain dependence of the storage modulus (G′) and loss modulus (G″) at a constant angular frequency ($\omega = 10$ Hz) (**a**), and frequency dependence of storage modulus (G′) and loss modulus (G″) at a constant strain (0.5 %) for Hyd and Hyd/clino samples (**b**)

8 wt%. The occurred phenomenon can be explained as follows. At clino contents less than 2 wt%, lower physical cross-linking density enables hydrogel to swell more. Besides, due to the special crystalline structure of clino with negative surface charges, high electrostatic repulsive forces between $-COO^-$ groups of hydrogel and negative surface charges of clino can result in enhanced expansion of hydrogel network and higher swelling ratio. However, at clino contents higher than 2 wt%, physical cross-linking density increases, resulting in the shrinked hydrogel network, and therefore reduced swelling ratio [32, 33]. On the other hand, high hydrophilicity of the hydrogel components compared to clino particles makes them most liable for water absorbency of the hydrogel nanocomposite. Consequently, high proportions of clino in the hydrogel composition will restrict the swelling capacity of the synthesized hydrogel nanocomposite. According to Fig. 6b, Hyd sample reached to own equilibrium water absorbency (677 g/g) within 3230 min, while in the case of Hyd/clino equilibrium water absorbency (1153 g/g) was achieved within 1500 min. Consequently, incorporation of clino into hydrogel network not only increased swelling ratio but also significantly improved the water uptake rate.

Swelling kinetics

Swelling kinetic of the hydrogel samples was studied using Voigt-based equation [34]:

$$S_t = S_e\left(1 - e^{-t/\tau}\right) \quad (7)$$

Where S_t (g/g) is swelling ratio at time t, S_e (g/g) is equilibrium swelling ratio, t (min) is swelling time, and τ (min) is the rate parameter. The rate parameter (τ) value is a measure of the swelling rate so that the hydrogel sample with low rate parameter will have high swelling rate. The Plot of $-\mathrm{Ln}\,(1 - S_t/S_e)$ against time (t) for Hyd and Hyd/clino samples yields straight lines (Fig. 7a), which their slopes give the rate parameters, as shown in Table 1. The rate parameters of Hyd and

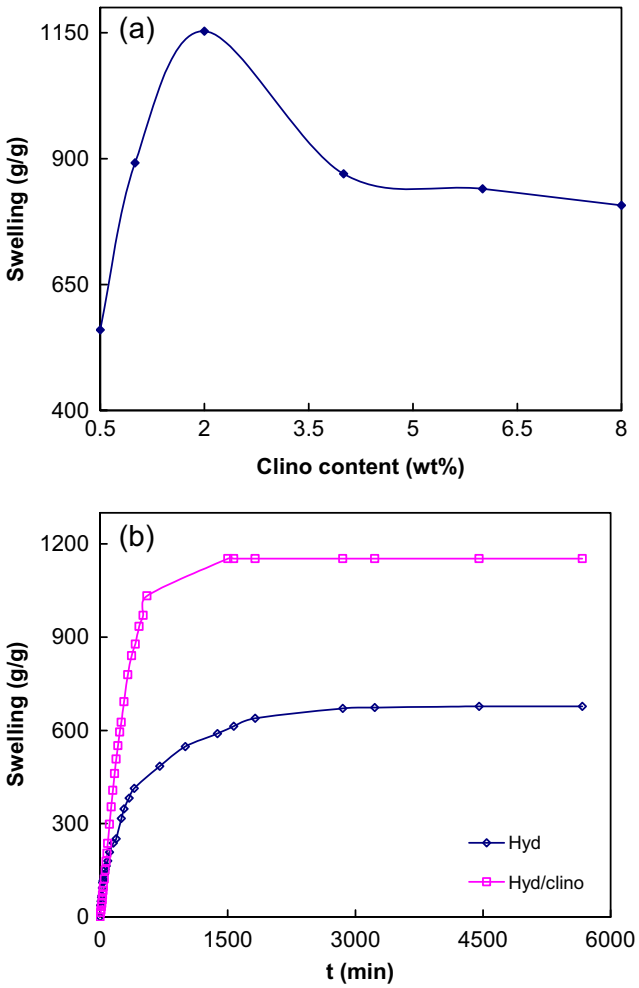

Fig. 6 The equilibrium water absorbency of hydrogel nanocomposite samples at different clino contents (**a**), and swelling kinetic diagrams of Hyd and Hyd/clino samples (**b**)

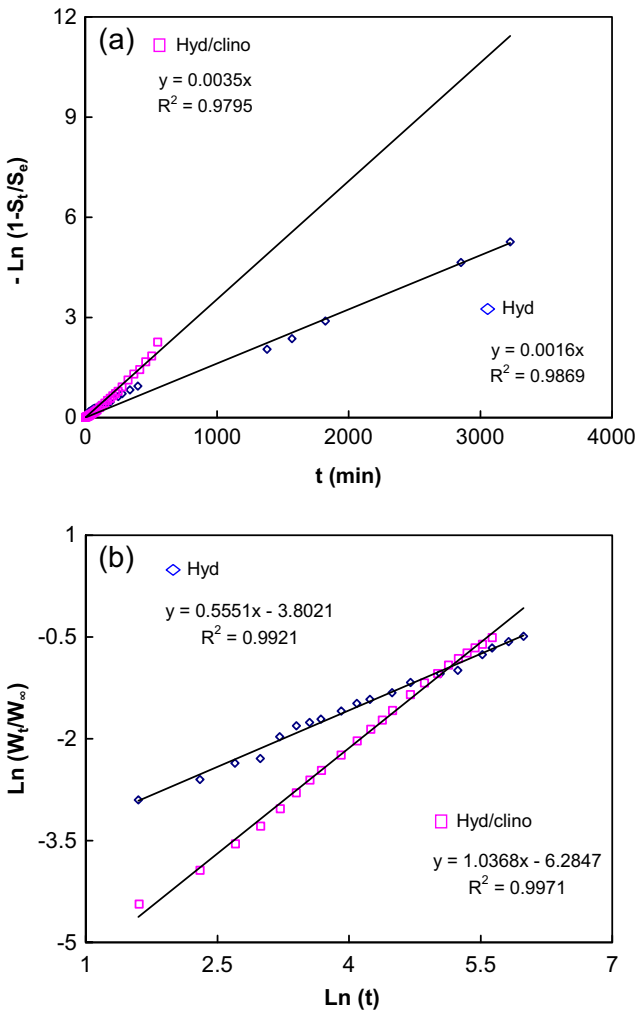

Fig. 7 Plots of $-\mathrm{Ln}\,(1 - S_t/S_e)$ versus t (**a**), and the plots of $\mathrm{Ln}\left(\frac{W_t}{W_\infty}\right)$ versus Ln (t) for Hyd and Hyd/clino samples (**b**)

Table 1 The swelling and diffusion parameters for Hyd and Hyd/clino samples

Sample	τ	n	k
Hydrogel (Hyd)	625	0.55	0.022
Hydrogel nanocomposite (Hyd/clino)	285.71	1.03	0.0018

Hyd/clino were 625 and 285.71 min, respectively, indicating the higher swelling rate of Hyd/clino compared with Hyd sample. To determine the nature of water diffusion into hydrogel network, swelling kinetic data obtained from first 60 % of the equilibrium water uptake were fitted to the following equation [35]:

$$\frac{W_t}{W_\infty} = kt^n \quad (8)$$

Where W_t and W_∞ are the swelling ratio of hydrogel at time t and at equilibrium, respectively. The k is a characteristic constant related to the structure of hydrogel network, and the exponent n determines the diffusion mechanism of the penetrant. When n is 0.5, the diffusion process complies with fickian diffusion mechanism. For n values between 0.5 and 1.0, the diffusion mechanism is non-fickian, for $n = 1.0$ the diffusion mechanism is case-II, and for $n > 1.0$, the diffusion mechanism is super case-II [21, 36]. The plot of $\mathrm{Ln}\left(\frac{W_t}{W_\infty}\right)$ versus $\mathrm{Ln}(t)$ for Hyd and Hyd/clino samples in distilled water yields straight lines, as shown in Fig. 7b. The exponents (n) and swelling constants (k) can be calculated from the slope and the intercept of the lines, respectively, which have been provided in Table 1. The value of n for Hyd and Hyd/clino samples was 0.55 and 1.03, respectively. Thus, water diffusion behavior of the hydrogel and hydrogel nanocomposite samples complies with the non-fickian and super case-II diffusion mechanism, respectively.

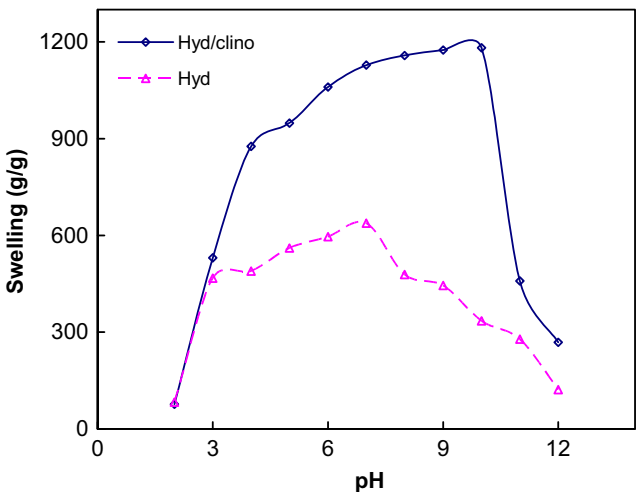

Fig. 8 The effect of pH on the equilibrium swelling ratio of Hyd and Hyd/clino samples

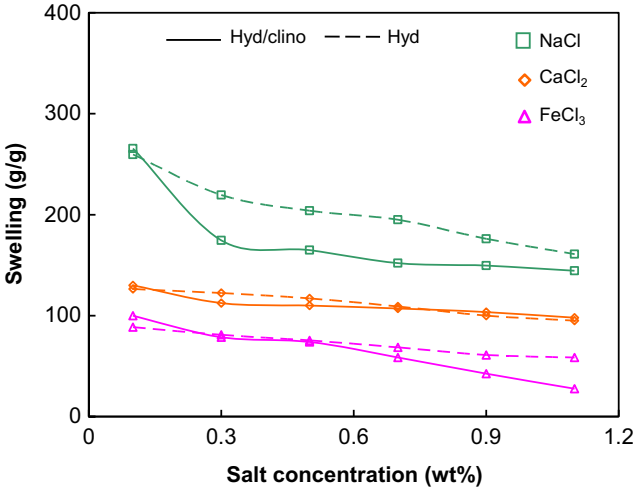

Fig. 9 The effect of salt solution type and concentration on the equilibrium swelling ratio of Hyd and Hyd/clino samples

Equilibrium swelling in solution of different pHs

The swelling behavior of the synthesized hydrogel samples at different pH values ranging from 2 to 12 has been demonstrated in Fig. 8. As can be seen for hydrogel sample, the swelling ratio increases considerably at pH values ranging from 2 to 5, and then rises gradually at pH values between 5 and 7 until it reaches to the highest value of 638 g/g at pH 7. Further increase in pH values to 12 results in the appreciable reduction of the swelling ratio. The observed trend of swelling capacity versus pH values can be explained as follows. In acidic media (pH < 5), higher physical cross-linking density caused by strong hydrogen-bonding interactions leads to the reduced swelling ratio. At pH values between 5 and 7, high dissociation degree of the carboxylate groups results in reinforcement of the electrostatic repulsions between carboxylate anions, and consequently enhanced swelling ratio. However, the lower swelling ratio in basic solutions (pH > 7) is due to the charge screening effect of excess Na^+ counterions in the swelling medium which shield the carboxylate anions and prevent effective anion-anion repulsions. In the case of superabsorbent nanocomposite, a similar trend of swelling ratio versus pH values is observed but its highest swelling capacity was achieved at pH 10. At this pH value, surface silanol groups of the clino particles are deprotonated which result in the increased electrostatic repulsions between $-SiO^-$ centers and carboxylate anions, and therefore highest swelling ratio. At pH values higher than 10, enhanced shielding effect of Na^+ counterions causes to shrinked hydrogel network, and thus reduced swelling capacity [21].

Effect of various saline solutions on swelling behavior

The equilibrium swelling behavior of the hydrogel samples in various saline solutions (NaCl, $CaCl_2$, and $FeCl_3$) with

different concentrations has been shown in Fig. 9. As depicted in Fig. 9, the equilibrium swelling ratio of hydrogel samples decreased as the concentration of saline solutions increased. This can be attributed to the charge screening effect of excess salt cations, causing non-perfect electrostatic repulsions between carboxylate anions. Besides, osmotic pressure difference between the polymer matrix and the swelling medium decreases with rising salt concentration leading to the reduced swelling capacity [37]. The swelling ratio of the hydrogel samples is also affected by type of the salt added to the external swelling medium. In the case of salt solutions with multivalent cations (Ca^{2+} and Fe^{3+}), ionic cross-linking points generated between carboxylate anions and cations cause an increase in cross-linking density, and consequently a substantial decrease in swelling ratio. Additionally, high electrostatic attraction between Fe^{3+} and carboxylate anions compared with the Ca^{2+} cations, results in a larger ionic cross-linking density, and therefore lower swelling ratio [38].

Study on fertilizer release behavior

The fertilizer release patterns of the untreated fertilizer compound (NPK), Hyd/NPK, and Hyd/clino/NPK formulations in water and also in soil have been exhibited in Fig. 10a and b, respectively. As shown in Fig. 10a, due to the ease of dissolution of NPK fertilizer compound in water, more than 90 % of fertilizer of untreated NPK compound released within 5 h. However, because of the barrier effect of polymeric matrix in hydrogel network, Hyd/NPK and Hyd/clino/NPK formulations showed a preferable sustained release property. The NPK fertilizer in Hyd/NPK and Hyd/clino/NPK formulations released 25.33, 49.05, 88.53 %, and 14.71, 32.92, and 72.86 % within first day, 1 week, and 1 month, respectively. According to Fig. 10b, the release profile of the untreated fertilizer compound in soil grew upward quickly until the amount of the released fertilizer reached 98 % within 4 h. In contrast, the release patterns of Hyd/NPK and Hyd/clino/NPK formulations in soil indicated more gentle manner which attained to almost constant levels within 30 days. The amount of fertilizer released from Hyd/NPK and Hyd/clino/NPK formulations was about 26.59, 46.94, 90.05 %, and 13.67, 29.75, and 77 % on the first day, 1 week, and 1 month, respectively. These findings showed that incorporation of clino particles into hydrogel network can cause hydrogel liberate fertilizer with a slower rate than that of neat hydrogel. The amount of the fertilizer released from Hyd/clino/NPK formulation did not exceed from 15 wt% on the first day and was not above 75 wt% on the 30th day. These results conform to the standard of slow-release fertilizers of the Committee of European Normalization (CEN), and thus Hyd/clino/NPK formulation has an excellent slow-release characteristic [39].

The fertilizer release mechanism of the NPK loaded hydrogel samples in soil can be explained as follows. The hydrogel sample would gradually absorb the soil water and transform into swollen state after being added into soil. Since, absorbed water molecules can flow in hydrogel network through interlinked pathways, therefore, dissolution of the encapsulated fertilizers would occur, slowly. Afterwards, the fertilizer

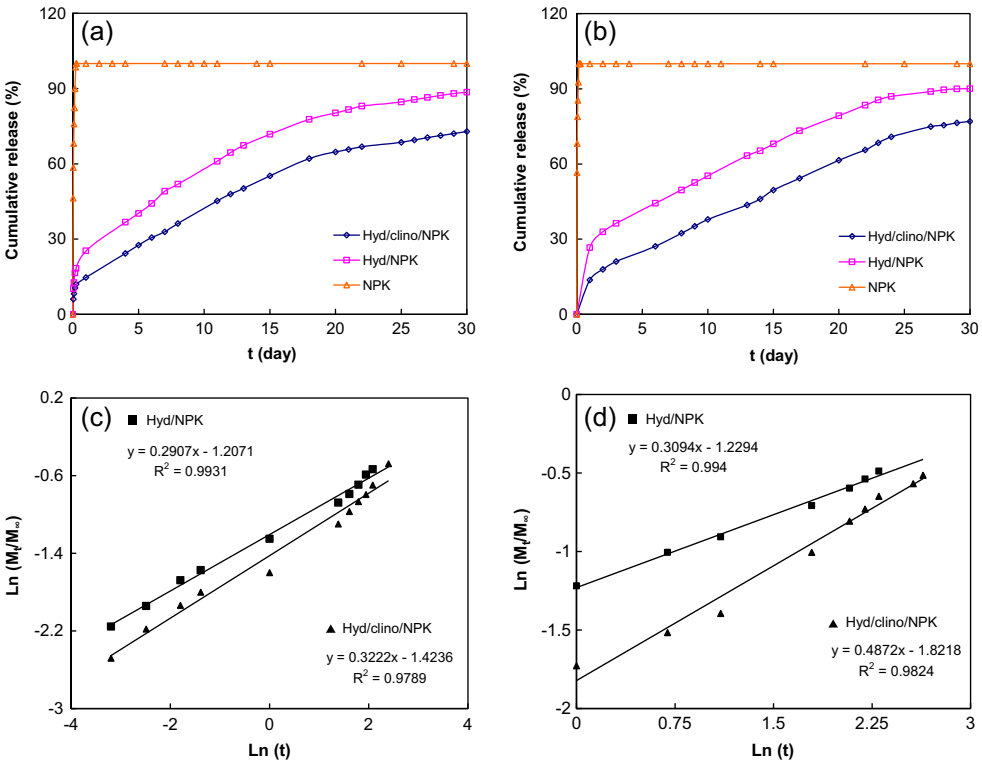

Fig. 10 Fertilizer release behaviors of untreated fertilizer (NPK), Hyd/NPK, and Hyd/clino/NPK formulations in distilled water (**a**), and in soil (**b**), and plots of Ln $\left(\frac{M_t}{M_\infty}\right)$ versus Ln (t) for Hyd/NPK and Hyd/clino/NPK formulations in distilled water (**c**), and in soil (**d**)

solution would diffuse out by dynamic exchange of water molecules between soil and hydrogel network. At this stage, diffusion can be the release rate-limiting step. The fertilizer release rate would increase with increasing the swelling ratio until it reaches to an almost constant level at equilibrium swelling state.

The SRF formulation developed in this work displays several advantages over the others which already have been described in the literature [40, 41]. First, SRF formulation was prepared by one step In-situ free-radical polymerization method in which additional steps such as coating of the fertilizer granules (coating procedure) did not require. Moreover, the use of clino as inorganic filler not only reduced final production cost of the prepared formulation but also greatly enhanced its water absorption capacity. Besides, incorporation of the clino into hydrogel network improved the nutrient-retention capability of the soil by promoting a slower release of the essential nutrients from fertilizer loaded hydrogels.

To determine the fertilizer release mechanism of Hyd/NPK and Hyd/clino/NPK formulations, the fertilizer release data were fitted with the following equation:

$$\frac{M_t}{M_\infty} = kt^n \quad (9)$$

Where M_t attributes to the amount of fertilizer released at time t, M_∞ is the total amount of fertilizer released at infinite time, t is the release time, k is a constant incorporating the structural and geometrical characteristics of the release device, and n is the release exponent indicating the type of fertilizer release mechanism. For $n \leq 0.5$ the fertilizer release follows a fickian diffusion mechanism. When n value is between 0.5 and 1.0 non-fickian diffusion mechanism is occurred, and For $n = 1.0$, fertilizer release mechanism is Case-II or zero-order type [42]. The plot of $\mathrm{Ln}\left(\frac{M_t}{M_\infty}\right)$ versus $\mathrm{Ln}(t)$ for Hyd/NPK and Hyd/clino/NPK formulations in distilled water (Fig. 10c) and also in soil (Fig. 10d) yields straight lines. The slope and intercept of these lines determine the values of n and k, respectively, which have been provided in Table 2. The values of n for Hyd/NPK and Hyd/clino/NPK formulations in distilled water were 0.29 and 0.32, respectively, indicating that the fertilizer release mechanism is fickian diffusion type for both formulations. For Hyd/NPK and Hyd/clino/NPK formulations in soil medium the n values were 0.3 and 0.48, respectively, indicating that the fertilizer release mechanism of the both formulations follows fickian diffusion type.

Table 2 The parameters of diffusion model for fertilizer release from Hyd/NPK and Hyd/clino/NPK formulations in distilled water and also in soil

Sample	Fertilizer release medium			
	Distilled water		Soil	
	n	k	n	k
Hyd/NPK	0.29	0.3	0.3	0.29
Hyd/clino/NPK	0.32	0.24	0.48	0.16

Water retention capability of Hyd/clino/NPK in soil

The preliminary evaluation of Hyd/clino/NPK formulation for water retention in loamy sand soil was performed and the results were shown in Fig. 11. Experimental results showed that all of the absorbed water in soil without Hyd/clino/NPK vaporized after 15 days, while soil with Hyd/clino/NPK maintained own water for a longer periods and its water retention capacity reached to 22.77 and 10.4 % on the 15th and 30th days, respectively. As a result, the use of Hyd/clino/NPK in soil can reduce irrigation frequencies and improve the ability of plants to fight against drought.

Conclusion

In summary, we synthesized a novel functional MB-based superabsorbent nanocomposite by In-situ free-radical graft copolymerization of acrylate-based monomers onto MB backbone in the presence of clino and NPK fertilizer compound. FTIR results showed that grafting of starch molecules onto acrylate monomers has been performed, successfully. To assess the gel framework stability of the synthesized three-dimensional cross-linked hydrogels, rheological analyses were carried out. The obtained results exhibited that both Hyd and Hyd/clino samples had a stable cross-linked gel networks. In addition, Hyd/clino sample presented higher gel strength compared with the neat hydrogel sample which arises

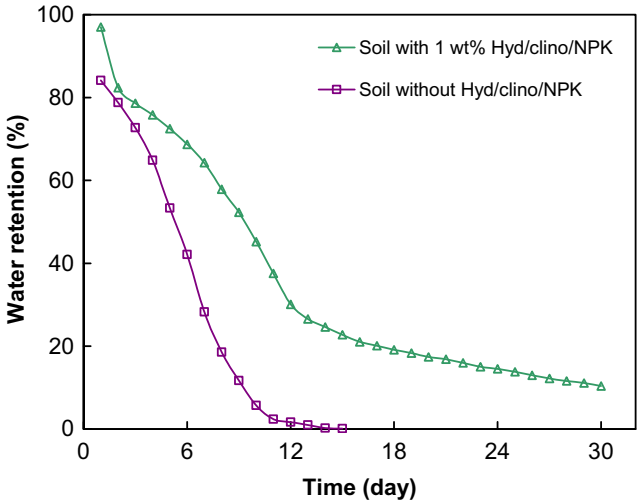

Fig. 11 Water-retention behavior of the loamy sand soil with and without Hyd/clino/NPK superabsorbent nanocomposite

from the physical crosslinking effect of clino particles. Water transport behavior of Hyd and Hyd/clino samples was determined by swelling kinetic studies. The swelling ratio of the hydrogel samples was affected by salt solution type and concentration, pH values, and clino contents. Fertilizer release results exhibited that Hyd/clino/NPK formulation has good slow-release property. Study on the fertilizer release kinetics of Hyd/NPK and Hyd/clino/NPK revealed that both formulations follow a fickian diffusional mechanism. Moreover, the Hyd/clino/NPK had good water retention capability in loamy sand soil. These findings suggest that the developed SRF formulation can efficiently improve the utilization of fertilizer and water resources in agricultural applications.

Acknowledgments We gratefully acknowledge the financial support of the University of Tabriz, Department of Applied Chemistry, Faculty of Chemistry, Tabriz, Iran.

References

1. Jin S, Yue G, Feng L, Han Y, Yu X, Zhang Z (2010) Preparation and properties of a coated slow-release and water-retention biuret phosphoramide fertilizer with superabsorbent. J Agric Food Chem 59(1):322–327
2. Guo M, Liu M, Zhan F, Wu L (2005) Preparation and properties of a slow-release membrane-encapsulated urea fertilizer with superabsorbent and moisture preservation. Ind Eng Chem Res 44(12): 4206–4211
3. Zhang J, Liu R, Li A, Wang A (2006) Preparation, swelling behaviors, and slow-release properties of a poly (acrylic acid-co-acrylamide)/sodium humate superabsorbent composite. Ind Eng Chem Res 45(1):48–53
4. Ni B, Liu M, Lu S, Xie L, Wang Y (2010) Multifunctional slow-release organic–inorganic compound fertilizer. J Agric Food Chem 58(23):12373–12378
5. Xie L, Liu M, Ni B, Zhang X, Wang Y (2011) Slow-release nitrogen and boron fertilizer from a functional superabsorbent formulation based on wheat straw and attapulgite. Chem Eng J 167(1):342–348
6. Tally M, Atassi Y (2015) Optimized synthesis and swelling properties of a pH-sensitive semi-IPN superabsorbent polymer based on sodium alginate-g-poly (acrylic acid-co-acrylamide) and polyvinylpyrrolidone and obtained via microwave irradiation. J Polym Res 22(9):1–13
7. Bardajee GR, Hooshyar Z (2013) Novel potentially biocompatible nanoporous hydrogel based on poly ((2-dimethylaminoethyl) methacrylate) grafted onto salep: synthesis, swelling behavior and drug release study. J Polym Res 20(1):1–8
8. Zhong K, Lin Z-T, Zheng X-L, Jiang G-B, Fang Y-S, Mao X-Y, Liao Z-W (2013) Starch derivative-based superabsorbent with integration of water-retaining and controlled-release fertilizers. Carbohydr Polym 92(2):1367–1376
9. Xie L, Liu M, Ni B, Wang Y (2012) Utilization of wheat straw for the preparation of coated controlled-release fertilizer with the function of water retention. J Agric Food Chem 60(28):6921–6928
10. Mahmoud GA, Abdel-Aal SE, Badway NA, Abo Farha SA, Alshafei EA (2014) Radiation synthesis and characterization of starch-based hydrogels for removal of acid dye. Starch 66(3–4): 400–408
11. Rodrigues FH, Fajardo AR, Pereira AG, Ricardo NM, Feitosa JP, Muniz EC (2012) Chitosan-graft-poly (acrylic acid)/rice husk ash based superabsorbent hydrogel composite: preparation and characterization. J Polym Res 19(12):1–10
12. Barkhordari S, Yadollahi M, Namazi H (2014) pH sensitive nanocomposite hydrogel beads based on carboxymethyl cellulose/layered double hydroxide as drug delivery systems. J Polym Res 21(6):1–9
13. Singh R, Singh D (2012) Radiation synthesis of PVP/alginate hydrogel containing nanosilver as wound dressing. J Mater Sci Mater Med 23(11):2649–2658
14. Ngadaonye JI, Geever LM, Killion J, Higginbotham CL (2013) Development of novel chitosan-poly (N, N-diethylacrylamide) IPN films for potential wound dressing and biomedical applications. J Polym Res 20(7):1–13
15. Wei Q-B, Fu F, Zhang Y-Q, Tang L (2015) Synthesis and characterization of pH-responsive carboxymethyl chitosan-g-polyacrylic acid hydrogels. J Polym Res 22(2):1–8
16. Zhang M, Cheng Z, Zhao T, Liu M, Hu M, Li J (2014) Synthesis, characterization, and swelling behaviors of salt-sensitive maize bran–poly (acrylic acid) superabsorbent hydrogel. J Agric Food Chem 62(35):8867–8874
17. Bortolin A, Aouada FA, Mattoso LH, Ribeiro C (2013) Nanocomposite PAAm/methyl cellulose/montmorillonite hydrogel: evidence of synergistic effects for the slow release of fertilizers. J Agric Food Chem 61(31):7431–7439
18. An J, Wang W, Wang A (2012) Preparation and swelling behavior of a pH-responsive psyllium-g-poly (acrylic acid)/attapulgite superabsorbent nanocomposite. Int J Polym Mater 61(12):906–918
19. Zaharia A, Sarbu A, Radu A-L, Jankova K, Daugaard A, Hvilsted S, Perrin F-X, Teodorescu M, Munteanu C, Fruth-Oprisan V (2015) Preparation and characterization of polyacrylamide-modified kaolinite containing poly [acrylic acid-co-methylene bisacrylamide] nanocomposite hydrogels. Appl Clay Sci 103:46–54
20. Kalaleh H-A, Tally M, Atassi Y (2015) Preparation of bentonite-g-poly (acrylate-co-acrylamide) superabsorbent polymer composite for agricultural applications: optimization and characterization. Polym Sci Ser B Polym Chem B 57(6):750–758
21. Rashidzadeh A, Olad A, Salari D, Reyhanitabar A (2014) On the preparation and swelling properties of hydrogel nanocomposite based on sodium alginate-g-Poly (acrylic acid-co-acrylamide)/clinoptilolite and its application as slow release fertilizer. J Polym Res 21(2):1–15
22. Rashidzadeh A, Olad A, Salari D (2015) The effective removal of methylene blue dye from aqueous solutions by NaAlg-g-poly (acrylic acid-co-acryl amide)/clinoptilolite hydrogel nanocomposite. Fibers Polym 16(2):354–362
23. Yang L, Ma X, Guo N, Zhang Y (2014) Preparation and characteristics of sodium alginate/Na^+ rectorite-g-itaconic acid/acrylamide hydrogel films. Carbohydr Polym 105:351–358
24. Gulrez SK, Phillips GO, Al-Assaf S (2011) Hydrogels: methods of preparation, characterisation and applications. INTECH Open Access Publisher
25. Yang L, Ma X, Guo N (2011) Synthesis and properties of sodium alginate/Na^+ rectorite grafted acrylic acid composite superabsorbent via 60 Coγ irradiation. Carbohydr Polym 85(2):413–418
26. Castaldi P, Santona L, Cozza C, Giuliano V, Abbruzzese C, Nastro V, Melis P (2005) Thermal and spectroscopic studies of zeolites exchanged with metal cations. J Mol Struct 734(1):99–105
27. Owens DE, Jian Y, Fang JE, Slaughter BV, Chen Y-H, Peppas NA (2007) Thermally responsive swelling properties of polyacrylamide/poly (acrylic acid) interpenetrating polymer network nanoparticles. Macromolecules 40(20):7306–7310
28. Moharram M, Balloomal L, El-Gendy H (1996) Infrared study of the complexation of poly (acrylic acid) with poly (acrylamide). J Appl Polym Sci 59(6):987–990

29. Rashidzadeh A, Olad A (2014) Slow-released NPK fertilizer encapsulated by NaAlg-g-poly (AA-co-AAm)/MMT superabsorbent nanocomposite. Carbohydr Polym 114:269–278
30. Larrubia MA, Ramis G, Busca G (2000) An FT-IR study of the adsorption of urea and ammonia over V_2O_5–MoO_3–TiO_2 SCR catalysts. Appl Catal B 27(3):L145–L151
31. Moura MJ, Figueiredo MM, Gil MH (2007) Rheological study of genipin cross-linked chitosan hydrogels. Biomacromolecules 8(12):3823–3829
32. Wu L, Liu M (2007) Slow-release potassium silicate fertilizer with the function of superabsorbent and water retention. Ind Eng Chem Res 46(20):6494–6500
33. Amnuaypanich S, Patthana J, Phinyocheep P (2009) Mixed matrix membranes prepared from natural rubber/poly (vinyl alcohol) semi-interpenetrating polymer network (NR/PVA semi-IPN) incorporating with zeolite 4A for the pervaporation dehydration of water–ethanol mixtures. Chem Eng Sci 64(23):4908–4918
34. Pourjavadi A, Jahromi PE, Seidi F, Salimi H (2010) Synthesis and swelling behavior of acrylatedstarch-g-poly (acrylic acid) and acrylatedstarch-g-poly (acrylamide) hydrogels. Carbohydr Polym 79(4):933–940
35. Alla SGA, Sen M, El-Naggar AWM (2012) Swelling and mechanical properties of superabsorbent hydrogels based on Tara gum/acrylic acid synthesized by gamma radiation. Carbohydr Polym 89(2):478–485
36. Rao KM, Mallikarjuna B, Krishna Rao K, Sudhakar K, Rao KC, Subha M (2013) Synthesis and characterization of pH sensitive poly (hydroxy ethyl methacrylate-co-acrylamidoglycolic acid) based hydrogels for controlled release studies of 5-fluorouracil. Int J Polym Mater Polym Biomater 62(11):565–571
37. Zhang J, Wang A (2007) Study on superabsorbent composites. IX: synthesis, characterization and swelling behaviors of polyacrylamide/clay composites based on various clays. React Funct Polym 67(8):737–745
38. Zheng Y, Li P, Zhang J, Wang A (2007) Study on superabsorbent composite XVI. Synthesis, characterization and swelling behaviors of poly (sodium acrylate)/vermiculite superabsorbent composites. Eur Polym J 43(5):1691–1698
39. Trenkel ME, Association IFI (1997) Controlled-release and stabilized fertilizers in agriculture, vol 11. International fertilizer industry association, Paris
40. Wu L, Liu M, Liang R (2008) Preparation and properties of a double-coated slow-release NPK compound fertilizer with superabsorbent and water-retention. Bioresour Technol 99(3):547–554
41. Ni B, Liu M, Lü S (2009) Multifunctional slow-release urea fertilizer from ethylcellulose and superabsorbent coated formulations. Chem Eng J 155(3):892–898
42. Ni B, Liu M, Lü S, Xie L, Zhang X, Wang Y (2010) Novel slow-release multielement compound fertilizer with hydroscopicity and moisture preservation. Ind Eng Chem Res 49(10):4546–4552